

**<sup>18</sup>F-FDG PET/MRI for staging and interim response assessment in pediatric and adolescent Hodgkin lymphoma: a prospective study with <sup>18</sup>F-FDG PET/CT as reference standard**

**Short running title**

PET/MRI in pediatric Hodgkin lymphoma

**Authors:**

Verhagen, Martijn V, MD 1,2	<a href="mailto:m.verhagen@umcg.nl">m.verhagen@umcg.nl</a>
Menezes, Leon J FRCP, FRCP 3,4	<a href="mailto:leon.menezes@nhs.net">leon.menezes@nhs.net</a>
Neriman, Deena, MB BS, FRCP 3	<a href="mailto:deena.neriman@nhs.net">deena.neriman@nhs.net</a>
Watson, Tom A, FRCP 2	<a href="mailto:tom.watson@gosh.nhs.uk">tom.watson@gosh.nhs.uk</a>
Punwani, Shonit, MRCP, FRCP, PhD 1	<a href="mailto:shonit.punwani@nhs.net">shonit.punwani@nhs.net</a>
Taylor, Stuart A, MRCP, FRCP, MD 1, 5	<a href="mailto:stuart.taylor1@nhs.net">stuart.taylor1@nhs.net</a>
Shankar, Ananth, MRCP, MD, FRCPCH 5, 6	<a href="mailto:ananth.shankar@nhs.net">ananth.shankar@nhs.net</a>
Daw, Stephen, FRCP 6	<a href="mailto:stephendaw@nhs.net">stephendaw@nhs.net</a>
Humphries, Paul D, MRCP, FRCP 1,2*	<a href="mailto:paul.humphries5@nhs.net">paul.humphries5@nhs.net</a>

\*Corresponding author

1 Department of Radiology

University College London Hospital, 235 Euston Road, London, UK NW1 2BU

2 Department of Radiology

Great Ormond St, London, UK WC1N 3JH

PET/MRI in pediatric Hodgkin lymphoma

3 UCL Institute of Nuclear Medicine

University College London Hospital, 235 Euston Road, London, UK NW1 2BU

4 NIHR University College London Hospitals Biomedical Research Centre

5 Centre for Medical Imaging, CBH

43-45 Foley Street, London, UK W1W 7TS

6 Department of pediatrics

University College London Hospital, 235 Euston Road, London, UK NW1 2BU

### **Disclaimer**

Funding was secured from Great Ormond Street Hospital Childrens' Charity.

### **First author**

Verhagen, Martijn V, MD. Pediatric radiologist

[m.verhagen@umcg.nl](mailto:m.verhagen@umcg.nl)

Phone: +31(0)625649708

Fax: +31 (050) 361 37 55

### **Address**

University Medical Center Groningen (UMCG)

Medical Imaging Center, EB44

Hanzeplein 1, 9713GZ Groningen

The Netherlands

**Corresponding author**

Humphries, Paul D, MRCP, FRCR 1,2\*

[paul.humphries5@nhs.net](mailto:paul.humphries5@nhs.net)

Address correspondence to:

Humphries, Paul D. Department of Radiology, University College London Hospital, 235

Euston Road, London, UK NW1 2BU

Tel: +44 (020) 7405 9200

Fax: +44 (020) 7813 8150

**Statement**

Funding was secured from Great Ormond Street Hospital Childrens' Charity.

## MANUSCRIPT

**Title:**  $^{18}\text{F}$ -FDG PET/MRI for staging and interim response assessment in pediatric and adolescent Hodgkin lymphoma: a prospective study with  $^{18}\text{F}$ -FDG PET/CT as reference standard

## ABSTRACT

### **Rationale:**

Treatment regimens for pediatric Hodgkin's lymphoma (HL) depend on accurate staging and treatment response assessment, based on accurate disease distribution and metabolic activity depiction. With the aim of radiation dose reduction, we compared the diagnostic performance of  $^{18}\text{F}$ -FDG PET/MR to a  $^{18}\text{F}$ -FDG PET/CT reference standard for staging and response assessment.

### **Methods:**

Twenty-four patients (mean age 15.4 years, range 8-19.5 years) with histologically proven HL were prospectively and consecutively recruited in 2015 and 2016, undergoing both  $^{18}\text{F}$ -FDG PET/CT and  $^{18}\text{F}$ -FDG PET/MRI at initial staging ( $N = 24$ ) and at response assessment ( $N = 21$ ). Diagnostic accuracy of  $^{18}\text{F}$ -FDG PET/MRI for both nodal and extra-nodal disease was compared to  $^{18}\text{F}$ -FDG PET/CT, which was considered as the reference standard. Discrepancies were retrospectively classified as perceptual or technical errors and  $^{18}\text{F}$ -FDG PET/MRI and  $^{18}\text{F}$ -FDG PET/CT were corrected by removing perceptual error. Agreement with Ann-Arbor staging and Deauville grading was also assessed.

**Results:**

For nodal and extranodal sites combined, corrected staging  $^{18}\text{F}$ -FDG PET/MRI sensitivity was 100% (95% confidence interval (CI) 96.7%-100%), specificity 99.5% (95%CI 98.3%-99.9%). Corrected response assessment  $^{18}\text{F}$ -FDG PET/MRI sensitivity was 83.3% (95%CI 36.5%-99.1%), specificity 100% (95%CI 99.2%-100%). Modified Ann-Arbor staging agreement between  $^{18}\text{F}$ -FDG PET/CT and  $^{18}\text{F}$ -FDG PET/MRI was perfect ( $k = 1.0$ ,  $p = 0.000$ ). Deauville grading agreement between  $^{18}\text{F}$ -FDG PET/MRI and  $^{18}\text{F}$ -FDG PET/CT was excellent ( $k = 0.835$ ,  $p = 0.000$ ).

**Conclusion:**

$^{18}\text{F}$ -FDG PET/MRI is a promising alternative to  $^{18}\text{F}$ -FDG PET/CT for staging and response assessment in children with Hodgkin lymphoma.

**Key words:**

Hodgkin lymphoma; PET-MRI; PET-CT; pediatric; staging

## INTRODUCTION

Hodgkin lymphoma (HL) is the most common childhood lymphoma, and one of the most common pediatric and adolescent cancers (1). Treatment outcomes are critically dependent on accurate imaging defined staging and thereafter, early treatment response assessments.

Staging consists of detection of anatomical locations of disease, using either CT or MRI, combined with metabolic assessment (2). This metabolic assessment consists of using  $^{18}\text{F}$ -2-deoxy-2-fluoro-D- glucose Positron Emission Tomography ( $^{18}\text{F}$ -FDG-PET) to detect increased glucose metabolism of lymphatic and extra-lymphatic tissue involved by HL (3). Imaging is repeated after two (for classical HL) or three (for lymphocyte predominant HL) cycles of chemotherapy to determine early response assessment, which determines if post-treatment radiotherapy is necessary (3). The decision to consolidate with radiotherapy is taken if there is either insufficient reduction in size of disease or if there is persistent abnormal metabolic activity. It is well established that the addition of  $^{18}\text{F}$ -FDG-PET to standard cross-sectional imaging improves accuracy for both initial staging and treatment response assessment, so most patients undergo repeated multi-modality imaging.

Both CT and  $^{18}\text{F}$ -FDG PET impart a significant radiation dose and repeated studies result in a cumulative dose associated with secondary malignancies (4,5). Children and young adults are particularly vulnerable to the long term effects of radiation and according to the linear no threshold model of radiation, any reduction in radiation exposure for this group would be beneficial (6,7). With hybrid  $^{18}\text{F}$ -FDG

PET/MRI systems now available and able to potentially replace  $^{18}\text{F}$ -FDG PET/CT with a single  $^{18}\text{F}$ -FDG PET/MRI (8,9), diagnostic radiation exposure could potentially be reduced by up to 80% (5,8,10), whilst maintaining both anatomical and metabolic information.

We aimed to test the hypothesis that  $^{18}\text{F}$ -FDG PET/MRI is an alternative to  $^{18}\text{F}$ -FDG PET/CT, for both staging and early response assessment. This was done by prospectively assessing and comparing the diagnostic performance of  $^{18}\text{F}$ -FDG PET/MRI against standard  $^{18}\text{F}$ -FDG PET/CT for initial staging and early response assessment in pediatric and adolescent patients with HL.

## MATERIALS AND METHODS

### **Patient Population**

This single centre prospective study was approved by the institutional review board, and written informed consent was obtained from either participant and/or guardians in all patients.

Patients were consecutively included between February 2015 and June 2016. Inclusion criteria were; histologically confirmed Hodgkin lymphoma, age 0-20 years, inclusion into the EuroNet PHL-C1 trial, LP1 trial or successor Euronet trials including Euronet PHL C2. Exclusion criteria were; previous HL, prior chemotherapy or radiotherapy, pregnancy, breastfeeding and contra-indications to MRI.

### **Summary of the Study**

As part of standard of care staging imaging at our institution, all patients underwent  $^{18}\text{F}$ -FDG PET/CT. The trial  $^{18}\text{F}$ -FDG PET/MRI was performed at the same

attendance as  $^{18}\text{F}$ -FDG PET/CT, using the same  $^{18}\text{F}$ -FDG injection, with the patient transferring to the  $^{18}\text{F}$ -FDG PET/MRI suite immediately after completion of the  $^{18}\text{F}$ -FDG PET/CT examination.

Following two (EuroNet PHL-C1) or three (EuroNet LP1) cycles of chemotherapy, disease was reassessed with  $^{18}\text{F}$ -FDG PET/CT and the trial  $^{18}\text{F}$ -FDG PET/MRI again performed immediately after the  $^{18}\text{F}$ -FDG PET/CT.  $^{18}\text{F}$ -FDG PET/CT was the standard of reference against which  $^{18}\text{F}$ -FDG PET/MRI was compared.

### **$^{18}\text{F}$ -FDG PET/CT Protocol**

$^{18}\text{F}$ -FDG PET/CT data was acquired using GE Discovery PET/CT in-line systems (General Electric Healthcare, Milwaukee, Wisconsin, USA) without time-of-flight (TOF) technology. Patients fasted for 6 hours, and hyperglycaemia ( $>10$  mmol/L) was excluded. A weight-adjusted dose of  $^{18}\text{F}$ -FDG was injected 60 minutes before imaging. Patients were scanned from skull vertex to mid-thigh level, at 3 minutes per bed position. CT was low dose for attenuation correction, acquisition parameters were adjusted according to patient weight. No intra-venous iodinated contrast was administered. Combined axial emission images of  $^{18}\text{F}$ -FDG PET and CT were reconstructed to a 128x128 resolution image, with 2.5mm slice thickness.

### **$^{18}\text{F}$ -FDG PET/MRI Protocol**

$^{18}\text{F}$ -FDG PET/MRI sequences were acquired on a hybrid 3 Tesla MR without TOF (Siemens Healthineers Biograph mMR, Erlangen, Germany). All sequences were acquired from skull vertex to mid-thigh level, at 5 minutes per bed position.

$^{18}\text{F}$ -FDG PET/MRI comprised of axial T2-HASTE (half-Fourier acquisition single-shot turbo spin-echo), axial and coronal TIRM (turbo inversion recovery



magnitude) sequences, and axial post Gadolinium T1 Dixon fat suppression sequences (TABLE 1). Four tissue class (soft tissue, fat, lung, air) attenuation correction maps were calculated from the two-point Dixon sequences. Combined axial emission images of  $^{18}\text{F}$ -FDG PET and T2-HASTE sequences were reconstructed to a 128x128 resolution image, with 5 mm slice thickness.

### **Analysis of Images**

All studies were read sequentially under trial conditions using Osirix workstation software (Osirix MD, Geneva, Switzerland) after all scans were performed. Readers were blinded to patient data, clinical data, and other modalities including the reference standard.

$^{18}\text{F}$ -FDG PET/CT scans were read by a nuclear medicine specialist (DN, 10 years dedicated nuclear medicine experience).  $^{18}\text{F}$ -FDG PET/MRI sequences were evaluated by a nuclear medicine specialist and pediatric radiologist in consensus (LM and PDH, both 15 years of experience).

Derivation of enhanced reference standard and correction for perceptual errors

Discrepancies between  $^{18}\text{F}$ -FDG PET/MRI and the  $^{18}\text{F}$ -FDG PET/CT reference standard were reviewed by an independent non-blinded pediatric radiologist (MV, 5 years dedicated pediatric radiology experience), using similar methodology to that of Latifoltojar et al (11). Minor discrepancies resulting from disease differently located at site boundaries were not labelled as discrepant. All other discrepancies were reviewed in consensus between MV and PH and assigned to error type 'perceptual' or 'technical'. Perceptual errors entailed retrospectively visible disease. A technical

error was noted for discrepancies unrelated to reader detection, such as difference in measured metabolic activity between  $^{18}\text{F}$ -FDG PET/MRI and  $^{18}\text{F}$ -FDG PET/CT.

Technical discrepancies were always considered in favour of the  $^{18}\text{F}$ -FDG PET/CT reference standard. By comparing datasets corrected for perceptual error we aimed to remove the human perception bias and better compare technical performance.

### **Staging Definitions**

Staging was performed according to the Cotswolds modified Ann Arbor classification (12,13). Nineteen nodal sites were assessed: cervical (left and right), anterior mediastinum, paratracheal, lung hilum (left and right), diaphragm, axilla (left and right), hepatic hilum, splenic hilum, spleen, coeliac trunk, para-aortic, mesenteric, iliac (left and right), inguinal (left and right). Ten extra-nodal sites were also registered: Lung, chest wall, kidneys, bone marrow, pleural, pericardium, bowel, stomach, liver and pancreas.

Nodal and extra-nodal disease involvement was defined as a focal area of  $\text{FDG}^{18}$  with a SUVmax (measured using a  $1\text{ cm}^2$  circular region of interest) uptake above mediastinal blood pool SUVmax (14) or FDG uptake greater than the surrounding background in a location incompatible with normal physiological activity (15,16). Nodal volumes were derived from measurements in 3 orthogonal dimensions (volume =  $1/6 \pi (a * b * c)$ ).

Any focal lung parenchymal  $^{18}\text{F}$ -FDG avid focus above mediastinal blood pool SUVmax was considered involved. As per EuroNet criteria, focal lung parenchymal

involvement was also considered involved in case of a focal consolidation, solitary nodule of greater than 1 cm or more than three sub-centimeter nodules.

Extra-nodal extension of disease was registered for contiguous extension of tissue beyond a nodal mass into adjacent structures.

Bone marrow involvement at staging was concluded if focal or multifocal FDG uptake was above that of the liver (17), at response assessment bone marrow involvement was defined as focal or multifocal higher uptake compared to normal marrow but reduced compared with baseline (with diffuse changes from chemotherapy allowed) (18). Bone marrow lesions on MRI were only considered as bone marrow involvement when combined with increased FDG uptake.

For response assessment each site was re-evaluated and residual metabolic activity classified using the 5-point Deauville scale (19).

### **Statistical Analysis**

Detection rates (sensitivity and specificity, with a 95% confidence interval) and area under the curve (AUC) were calculated for nodal and extra-nodal sites combined.  $^{18}\text{F}$ -FDG PET/MRI was subsequently compared to  $^{18}\text{F}$ -FDG PET/CT as reference standard; with and without correction for perceptual error.

The kappa statistic was determined to test agreement between modalities. This was classified as poor for  $\kappa < 0.00$ ; slight for  $\kappa 0.00\text{--}0.20$ ; fair for  $\kappa 0.21\text{--}0.40$ ; moderate for  $\kappa 0.41\text{--}0.60$ ; good for  $\kappa 0.61\text{--}0.80$ ; and excellent for  $\kappa 0.81\text{--}1.00$  (20).

Individual nodal volume and individual SUVmax of nodal and extra-nodal sites were compared between  $^{18}\text{F}$ -FDG PET/MRI and  $^{18}\text{F}$ -FDG PET/CT at staging and response assessment. Correlation was calculated using Spearman's correlation test.

Statistics were performed using SPSS for Windows (release 26, IBM, New York, United States of America). The level of significance was set at  $\alpha < 0.05$ .

## RESULTS

Twenty-six patients were recruited (male:female ratio 14:12, median age 16, range 8-19 years). After exclusion, 24 patients were enrolled for staging, and 21 remained also for response assessment. Twenty-two patients had histologically confirmed classic HL, two had nodular lymphocyte predominant HL. The study flowchart is presented in FIGURE 1.

The median time between  $^{18}\text{F}$ -FDG injection and  $^{18}\text{F}$ -FDG PET/CT was 68 minutes (interquartile range (IQR) 16). Median interval time between  $^{18}\text{F}$ -FDG PET/CT and  $^{18}\text{F}$ -FDG PET/MRI was 95 minutes (IQR 35.5).

### Staging

$^{18}\text{F}$ -FDG PET/CT detected 141 disease positive sites (136/456 nodal, 5/240 extranodal: 696 sites total) (TABLE 2). The modified Ann Arbor stage distribution was: stage 1, 1 patient (1/24: 4.2%); stage 2, 13 patients (13/24: 54.2%); stage 3, 6 patients (6/24: 25%), stage 4, 4 patients (4/24: 16.7%).

$^{18}\text{F}$ -FDG PET/MRI detected 135 out of 141 true positive sites, 551 true negative sites, 4 false positive sites, and 6 false negatives (TABLE 2). Six out of 6 false negative sites were because of perceptual error. Three out of 4 false positive sites were because of technical errors, these false positive sites were small in volume (0.02-1.3ml) but  $^{18}\text{F}$ -FDG avid, whereas they were not  $^{18}\text{F}$ -FDG avid on the  $^{18}\text{F}$ -FDG

PET/CT reference standard. The remaining single false positive site was because of perceptual error (TABLE 2).

Uncorrected and corrected sensitivity and specificity are given in TABLE 3. <sup>18</sup>F-FDG PET/MRI intermodality agreement for disease sites compared to <sup>18</sup>F-FDG PET/CT detection was excellent for both uncorrected and corrected data (TABLE 3).

There were no discrepancies between <sup>18</sup>F-FDG PET/MRI and <sup>18</sup>F-FDG PET/CT for modified Ann Arbor staging (TABLE 4). Figure 2 demonstrates an involved nodal site at staging, which was concordant between <sup>18</sup>F-FDG PET/CT and <sup>18</sup>F-FDG PET/MRI.

### **Response Assessment**

At response assessment, <sup>18</sup>F-FDG PET/CT demonstrated 6 incomplete metabolic response sites (4/399 nodal and 2/210 extranodal: 609 sites total) in 3 out of 21 patients (TABLE 2). Deauville grade distribution was: grade 2, 11 patients (11/21: 52.4%); grade 3, 7 patients (7/21: 33.3%); grade 4, 3 patients (3/21: 14.3%). Figure 3 demonstrates <sup>18</sup>F-FDG PET/MR of nodal site involvement at staging and response assessment.

<sup>18</sup>F-FDG PET/MRI correctly detected 5/6 incomplete metabolic response sites, 1 incomplete metabolic response site was not detected due to a technical error (Deauville 3 on <sup>18</sup>F-FDG PET/MRI compared to Deauville 4 on <sup>18</sup>F-FDG PET/CT). There were no perceptual errors. Uncorrected and corrected sensitivity and specificity are given in TABLE 3.

Intermodality agreement for disease sites between  $^{18}\text{F}$ -FDG PET/MRI and  $^{18}\text{F}$ -FDG PET/CT detection was excellent (TABLE 3).  $^{18}\text{F}$ -FDG PET/MRI response assessment according to Deauville was excellent (TABLE 4).

### **Extra-Nodal Disease**

At staging 5/141 involved sites were extranodal (3 bone marrow sites, and 2 lung sites). Regarding the lung sites, one patient had one lung nodule measuring 12 and 14 mm on T2-HASTE and CT, respectively. The other patient had multiple lung nodules: 12 nodules were detected on T2-HASTE measuring up to 14 mm, and 41 nodules measuring up to 18 mm on CT.

At response assessment 2 incomplete metabolic response sites were extranodal (one bone marrow and one lung site). Further statistical analyses was omitted due to the low number of extranodal sites.

### **Volume**

At staging, correlation between individual nodal disease sites volumes at  $^{18}\text{F}$ -FDG PET/MRI and  $^{18}\text{F}$ -FDG PET/CT was excellent ( $r$  0.817,  $p$  = 0.000). Volumes are given in TABLE 5.

At response assessment, correlation was good ( $r$  0.728,  $p$  = 0.000). Volumes and volume reduction percentages at response assessment are given in TABLE 5.

### **SUVmax**

At staging, there was good correlation ( $r$  0.732,  $p$  = 0.000) between SUVmax from  $^{18}\text{F}$ -FDG PET/MRI and  $^{18}\text{F}$ -FDG PET/CT, SUVmax values are given in TABLE 5.

Correlation at response assessment was moderate ( $r = 0.543$ ,  $p = 0.000$ ), SUVmax values are given in TABLE 5.

## DISCUSSION

This study prospectively compared  $^{18}\text{F}$ -FDG PET/MRI to  $^{18}\text{F}$ -FDG PET/CT for both staging and early post-chemotherapy response reassessment in a cohort of children and adolescents with Hodgkin Lymphoma.

By comparing the diagnostic performance of these modalities, we wanted to test the hypothesis that  $^{18}\text{F}$ -FDG PET/MRI is an alternative to  $^{18}\text{F}$ -FDG PET/CT in pediatric HL, with the aim of reducing the cumulative radiation dose that these children receive throughout their illness. To correct for human perception bias, we present data corrected and uncorrected for perceptual error. Technical error due to differences in technique was not corrected for.

When corrected for perceptual error our results showed perfect agreement for modified Ann Arbor staging between  $^{18}\text{F}$ -FDG PET/MRI and  $^{18}\text{F}$ -FDG PET/CT, and excellent response assessment agreement according to the Deauville scale. The notion that  $^{18}\text{F}$ -FDG PET/MRI may replace  $^{18}\text{F}$ -FDG PET/CT is further supported by good to excellent intermodality correlation of SUVmax and nodal sizes at staging, and moderate to good correlation at response assessment.

In adults, excellent to perfect staging agreement ( $k = 0.979-1.0$ ) between  $^{18}\text{F}$ -FDG PET/CT and  $^{18}\text{F}$ -FDG PET/MRI for staging of mixed groups of Hodgkin and non-Hodgkin lymphoma has been reported (13,21,22). However, given the differences in body habitus, physiology (e.g. brown fat), the challenges of prolonged MRI protocols in children, and possibly different behaviour of lymphomas, adult

studies comparing  $^{18}\text{F}$ -FDG PET/MRI with  $^{18}\text{F}$ -FDG PET/CT cannot be extrapolated to children and adolescents (4,11,23). Those available pediatric studies comparing  $^{18}\text{F}$ -FDG PET/MRI and  $^{18}\text{F}$ -FDG PET/CT have so far consisted of a mix of both Hodgkin and non-Hodgkin lymphoma, and studied either staging or response assessment (4,24). Our study aimed to improve on the pediatric literature by prospectively including only pediatric HL and studying both staging and early response assessment.

Because of a longer study duration, a smaller bore diameter, and loud noises, undergoing  $^{18}\text{F}$ -FDG PET/MRI instead of  $^{18}\text{F}$ -FDG PET/CT may be challenging for some children (and adults). Preparation using virtual reality glasses, a mock MRI and play specialists may help children to be comfortable in an MRI (25). However, diagnostic performance must have priority over reduction of radiation dose. For those children unable to lie still in the MRI, either anesthesia or  $^{18}\text{F}$ -FDG PET/CT instead of  $^{18}\text{F}$ -FDG PET/MRI may be necessary.

In addition to reduced radiation dose, replacing  $^{18}\text{F}$ -FDG PET/MRI with  $^{18}\text{F}$ -FDG PET/CT may have another benefit. MRI sequences have intrinsic superior soft tissue contrast compared to CT, and this may allow for better delineation of lymph nodes (e.g. hilar lymph nodes) and focal solid organ lesion. However, although lung nodules can be seen on MRI, CT has superior air to tissue contrast, and a diagnostic chest CT is advised at staging of lung nodules (26). Consequently, our current practise consists of  $^{18}\text{F}$ -FDG PET/MRI at staging and response assessment, in combination with a diagnostic non-contrast enhanced chest CT at staging in all



patients, and at response assessment in those children with lung involvement at staging.

A limitation of this study was the necessity to scan and then move the patients between the  $^{18}\text{F}$ -FDG PET/CT and  $^{18}\text{F}$ -FDG PET/MRI. This was again unavoidable where ethics allows only one  $^{18}\text{F}$ -FDG injection.

The effects of delay between injection and PET scanning are twofold. The first is reduction in  $^{18}\text{F}$ -FDG activity due to decay of the isotope, which may influence SUV measurements. The second is prolonged uptake time, which may increase the detection of disease locations due to washout in normal structures and higher activity in some disease sites due to slow tracer uptake (27). There are published examples of this phenomenon, for example false negative  $^{18}\text{F}$ -FDG PET/CT but true positive  $^{18}\text{F}$ -FDG PET/MRI adrenal lesions (13), which were thought to be the result of prolonged uptake time.

Although we found no difference in staging between  $^{18}\text{F}$ -FDG PET/MRI and  $^{18}\text{F}$ -FDG PET/CT at diagnosis, there were site discrepancies which could have a potential clinical impact for children requiring radiotherapy. These discrepancies, regarded in our study as technical errors, may be due to the delayed  $^{18}\text{F}$ -FDG PET/MRI compared to  $^{18}\text{F}$ -FDG PET/CT. In our study, three (small volume: range 0.02-1.3ml) sites were considered false positive on  $^{18}\text{F}$ -FDG PET/MRI at staging due to higher SUVmax on  $^{18}\text{F}$ -FDG PET/MRI compared to  $^{18}\text{F}$ -FDG PET/CT. Although the reason for this cannot be verified, we postulate that this discrepancy may be related to the prolonged uptake time on the  $^{18}\text{F}$ -FDG PET/MRI. Conversely, differences in perfusion and washout may also account for the lower Deauville scale measurement of 2 sites on  $^{18}\text{F}$ -FDG PET/MRI during response assessment.

Lastly, there were only 6 sites at response assessment which did not show complete metabolic response. Although there was excellent agreement of  $^{18}\text{F}$ -FDG PET/MRI compared to  $^{18}\text{F}$ -FDG PET/CT at response assessment, these numbers are too small to draw definitive conclusions. Further studies to confirm these findings should include a larger population, which may be feasible especially in a multi-center collaboration.

## CONCLUSION

In our cohort of patients,  $^{18}\text{F}$ -FDG PET/MRI showed no difference in overall staging compared to  $^{18}\text{F}$ -FDG PET/CT for staging of HL in children and adolescents, and there was excellent response assessment agreement. With the aim of reducing cumulative radiation dose, we suggest that pediatric/adolescent HL staging and response assessment may be performed using  $^{18}\text{F}$ -FDG PET/MRI instead of  $^{18}\text{F}$ -FDG PET/CT, wherever possible.

## KEY POINTS

### QUESTION:

- Can  $^{18}\text{F}$ -FDG PET/MRI replace  $^{18}\text{F}$ -FDG PET/CT for staging and response assessment of pediatric Hodgkin lymphoma?

### PERTINENT FINDINGS:

- This prospective observational study demonstrates that  $^{18}\text{F}$ -FDG PET/MRI is a promising alternative to  $^{18}\text{F}$ -FDG PET/CT for staging and chemotherapy response assessment for pediatric Hodgkin lymphoma.

### IMPLICATIONS FOR PATIENT CARE:

- By replacing  $^{18}\text{F}$ -FDG PET/CT with  $^{18}\text{F}$ -FDG PET/MRI, children with Hodgkin lymphoma will receive a lower cumulative radiation dose at staging and response assessment, whilst maintaining diagnostic accuracy.

## DISCLOSURES

Funding was secured from Great Ormond Street Hospital Childrens' Charity.

None of the authors have any potential financial conflict of interest related to this manuscript.

## REFERENCES

1. Ward E, DeSantis C, Robbins A, Kohler B, Jemal A. Childhood and Adolescent Cancer Statistics. *Ca Cancer J Clin.* 2014;64:83-103.
2. Gallamini A, Hutchings M, Ramadan S. Seminars in Hematology. *Semin Hematol.* 2016;53:148-154.
3. Kluge R, Kurch L, Georgi T, Metzger M. Current Role of FDG-PET in Pediatric Hodgkin's Lymphoma. *Semin Nucl Med.* 2017;47:242-257.
4. Sher AC, Seghers V, Paldino MJ, et al. Assessment of sequential PET/MRI in comparison with PET/CT of Pediatric Lymphoma: A prospective Study. *Am J Roentgenol.* 2016;206:623-631.
5. Chawla SC, Federman N, Zhang D, et al. Estimated Cumulative Radiation Dose from PET / CT in Children with Malignancies : a 5-Year Retrospective Review. *Pediatr Radiol.* 2010;40:681-686.
6. Goske MJ, Applegate KE, Bulas D, et al. Image Gently: Progress and Challenges in CT Education and Advocacy. *Pediatr Radiol.* 2011;41:461.
7. Pearce MS. Patterns in paediatric CT use: An international and epidemiological perspective. *J Med Imaging Radiat Oncol.* 2011;55:107-109.
8. Hirsch FW, Sattler B, Sorge I, et al. PET/MR in children. Initial Clinical Experience in Paediatric Oncology using an Integrated PET/MR Scanner. *Pediatr Radiol.* 2013;43:860-875.
9. Schäfer JF, Gatidis S, Schmidt H, et al. Simultaneous Whole-Body PET/MR Imaging in Comparison to PET/CT in Pediatric Oncology: Initial Results. *Radiology.* 2014;273:220-231.
10. Li Y, Jiang L, Wang H, Cai H, Xiang Y, Li L. Effective Radiation Dose of 18F-

FDG PET/CT: How Much Does Diagnostic CT Contribute? *Radiat Prot Dosimetry*. 2019;187:183-190.

11. Latifoltojar A, Punwani S, Lopes A, et al. Whole-body MRI for Staging and Interim Response Monitoring in Paediatric and Adolescent Hodgkin's Lymphoma: a Comparison with Multi-Modality Reference Standard including 18F-FDG-PET-CT. *Eur Radiol*. 2018:1-11.
12. Lister TA, Crowther D, Sutcliffe SB, et al. Report of a Committee convened to discuss the Evaluation and Staging of Patients with Hodgkin's Disease: Cotswolds Meeting. *J Clin Oncol*. 1989;7:1630-1636.
13. Afaq A, Fraioli F, Sidhu H, et al. Comparison of PET/MRI with PET/CT in the Evaluation of Disease Status in Lymphoma. *Clin Nucl Med*. 2017;42:1-7.
14. Elstrom R, Guan L, Baker G, et al. Utility of FDG-PET scanning in Lymphoma by WHO Classification. *Blood*. 2003;101:3875-3876.
15. Kleis M, Daldrup-Link H, Matthay K, et al. Diagnostic Value of PET/CT for the Staging and Restaging of Pediatric Tumors. *Eur J Nucl Med Mol Imaging*. 2009;36:23-36.
16. Punwani S, Taylor SA, Bainbridge A, et al. Pediatric and Adolescent Lymphoma : Comparison of Whole-Body STIR Half-Fourier RARE MR Imaging with an Enhanced PET/CT Reference for Initial Staging. *Radiology*. 2010;255:182-90.
17. Adams HJA, Kwee TC, de Keizer B, et al. Systematic Review and Meta-Analysis on the Diagnostic Performance of FDG-PET/CT in detecting Bone Marrow Involvement in newly diagnosed Hodgkin Lymphoma: is Bone Marrow Biopsy still necessary? *Ann Oncol*. 2014;25:921-927.
18. Barrington SF, Kluge R. FDG PET for Therapy monitoring in Hodgkin and non-

- Hodgkin Lymphomas. *Eur J Nucl Med Mol Imaging*. 2017;44:97-110.
19. Meignan M, Gallamini A, Meignan M, Gallamini A, Haioun C. Report on the First International Workshop on interim-PET scan in lymphoma. *Leuk Lymphoma*. 2009;50:1257-1260.
  20. Landis JR, Koch GG. The Measurement of Observer Agreement for Categorical Data. *Biometrics*. 1977;33:159.
  21. Heacock L, Weissbrot J, Raad R, et al. PET/MRI for the Evaluation of Patients With Lymphoma: Initial Observations. *Am J Roentgenol*. 2015;204:842-848.
  22. Kirchner J, Deuschl C, Grueneisen J, et al. 18F-FDG PET/MRI in Patients suffering from Lymphoma: how much MRI Information is really needed? *Eur J Nucl Med Mol Imaging*. 2017;44:1005-1013.
  23. States LJ, Reid JR. Whole-body PET/MRI Applications in Pediatric Oncology. *Am J Roentgenol*. 2020;215:713-725.
  24. Ponisio MR, Mcconathy J, Laforest R, Khanna G. Evaluation of Diagnostic Performance of Whole-Body simultaneous PET / MRI in Pediatric Lymphoma. *Pediatr Radiol*. 2016:1258-1268.
  25. Edwards AD, Arthurs OJ. Paediatric MRI under Sedation: is it necessary? What is the Evidence for the Alternatives? *Pediatr Radiol*. 2011;41:1353-1364.
  26. Cieszanowski A, Lisowska A, Dabrowska M, et al. MR Imaging of Pulmonary Nodules: Detection Rate and accuracy of Size Estimation in Comparison to Computed Tomography. *PLoS One*. 2016;11:1-11.
  27. Al-Nabhani KZ, Syed R, Michopoulou S, et al. Qualitative and Quantitative Comparison of PET/CT and PET/MR Imaging in Clinical Practice. *J Nucl Med*. 2014;55:88-94.

TABLE 1. MRI sequences

	TIRM	Dixon	T2-HASTE	3D VIBE
Scanning plane	axial/cor	axial	axial	axial (liver and spleen)
Fat suppression	yes	yes	no	yes
Inversion time (ms)	220	N/A	N/A	180
Gadolinium-chelate	N/A	yes	N/A	0, 30, 60 sec
Echo Time (ms)	56	1.23, 2.46	92	1.91
Repetition Time (ms)	6870	4.1	1500	4.3
Flip Angle (degrees)	135	9	102	9
Section Thickness (mm)	7/4	3	5	3.5
Spacing (mm)	8.75/5.20	0	6	0
B-value s/mm <sup>2</sup>				
Echo train	11	1	256	1
Pixel space (mm)	1.76 x 1.76	0.78 x 0.78	1.02 x 1.02	1.19 x 1.19
Resolution (voxel)	256 x 176	640 x 500	448 x 336	320 x 260

Cor: coronal

HASTE: half-Fourier acquisition single-shot turbo spin-echo

mm: millimetre

ms: milliseconds

N/A: not applicable

TIRM: turbo inversion recovery magnitude

VIBE: volumetric interpolated breath-hold examination

TABLE 2. Technical and perceptual errors, nodal and extra-nodal sites combined

	Staging		Response assessment	
	<sup>18</sup> F-FDG	<sup>18</sup> F-FDG	<sup>18</sup> F-FDG	<sup>18</sup> F-FDG
	PET/CT(n)	PET/MRI(n)	PET/CT(n)	PET/MRI(n)
TP	141	135	6	5
FP	N/A	4	0	0
- <i>FP perceptual</i>			1	0
- <i>FP technical</i>			3	0
TN	560	551	603	603
FN	N/A	6	0	1
- <i>FN perceptual</i>			6	0
- <i>FN technical</i>			0	1
Total number of sites	696	696	609	609

FN: false negative; FP: false positive; N/A: not applicable; n: number of patients;

TN: true negative; TP: true positive



TABLE 3. <sup>18</sup>F-FDG PET/MRI detection of involved sites

	Uncorrected for perceptual error	Corrected for perceptual error
<b>Staging</b>		
Sensitivity	95.7% (135/141, 95%CI 90.6%-98.3%)	100% (141/141/ 95%CI 96.7%-100%)
Specificity	99.3% (551/555, 95%CI 98.0%-99.8%)	99.5% (552/555, 95%CI 98.3%-99.9%)
Kappa	0.960 (p = 0.000)	0.987 (p = 0.000)
AUC	0.979 (p = 0.000)	0.997 (p = 0.000)
<b>Response assessment</b>		
Sensitivity	83.3% (5/6, 95%CI 36.5%-99.1%)	N/A
Specificity	100% (603/603, 95%CI 99.2%-100%)	N/A
Kappa	0.908 (p = 0.000)	N/A
AUC	0.917 (p = 0.000)	N/A

AUC: area under the curve; 95%CI: 95% confidence interval; N/A: not applicable in absence of perceptual errors at response assessment

TABLE 4. Staging and early response assessment, agreement of <sup>18</sup>F-FDG PET/MRI compared to <sup>18</sup>F-FDG PET/CT

	<sup>18</sup> F-FDG PET/MRI
<u>Staging (N = 24)</u>	
Concordant	24
Upstaged	0
Downstaged	0
Intermodality agreement (kappa)	1.0 (p = 0.000)
<u>Response (N = 21)</u>	
Concordant	19
Higher Deauville	0
Lower Deauville	2*
Intermodality agreement (kappa)	0.835 (p = 0.000)

\*One case because of Deauville 3 instead of 4, and one because of Deauville 2 instead of 3

N = number

TABLE 5. Volume and SUVmax per individual nodal sites

	<sup>18</sup> F-FDG PET/MRI	<sup>18</sup> F-FDG PET/CT
<u>Volume</u>		
<u>Staging</u>		
Median, ml (IQR)	6.5 (19.2)	8.3 (26.7)
<u>Response</u>		
Median, ml (IQR)	1.4 (2.9)	1.8 (5.7)
Volume reduction, %	86.90	80.35
<u>SUVmax, mg/ml</u>		
<u>Staging</u>		
Median, mg/ml (IQR)	8.0 (4.8)	8.2 (4.8)
<u>Response</u>		
Median, mg/ml (IQR)	1.2 (0.6)	1.7 (0.7)

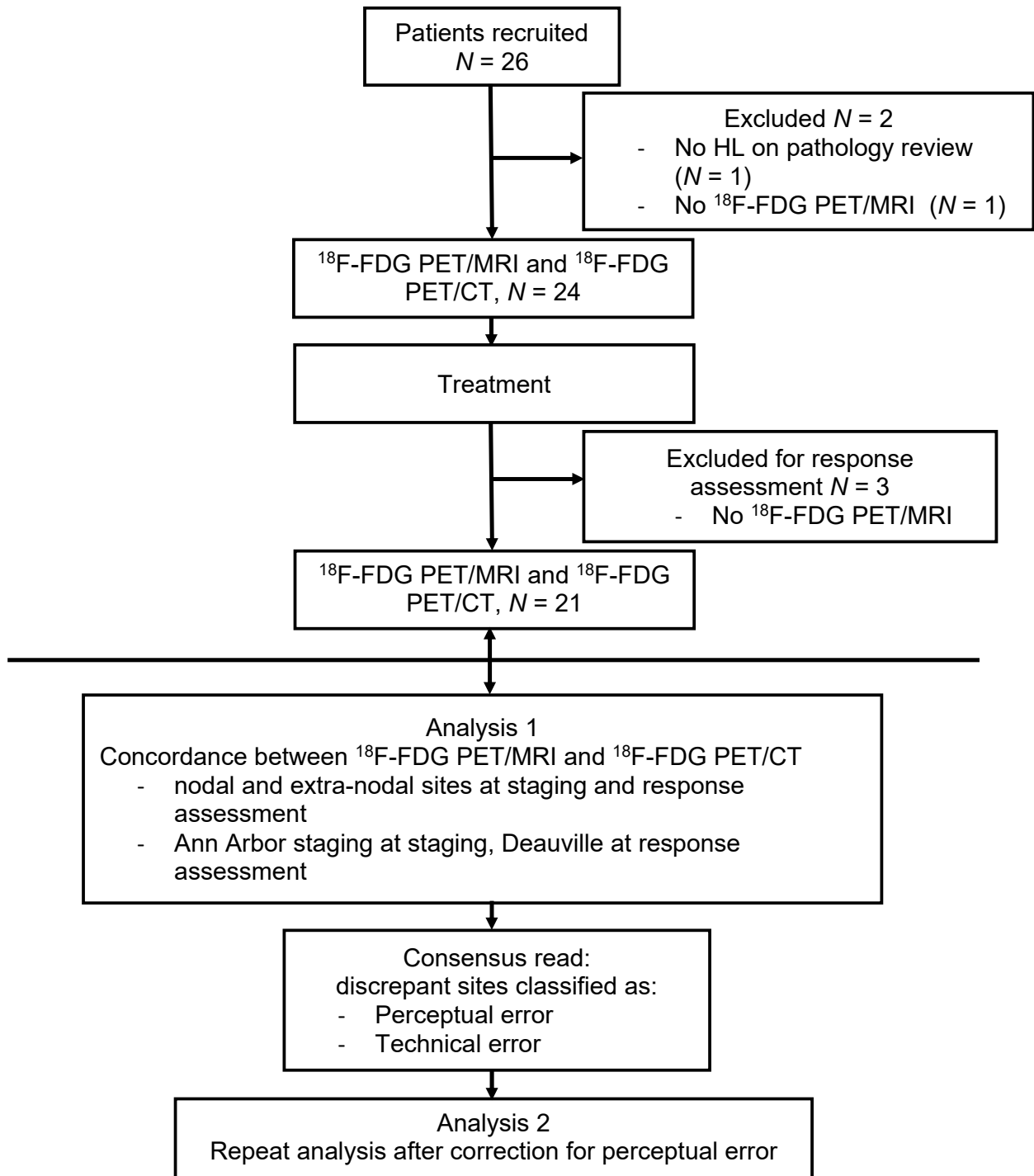
IQR: Interquartile range; N/A: Not applicable; SD: Standard deviation;

SUVmax: maximum standard uptake value

FIGURE LEGENDS

FIGURE 1

Study Flowchart



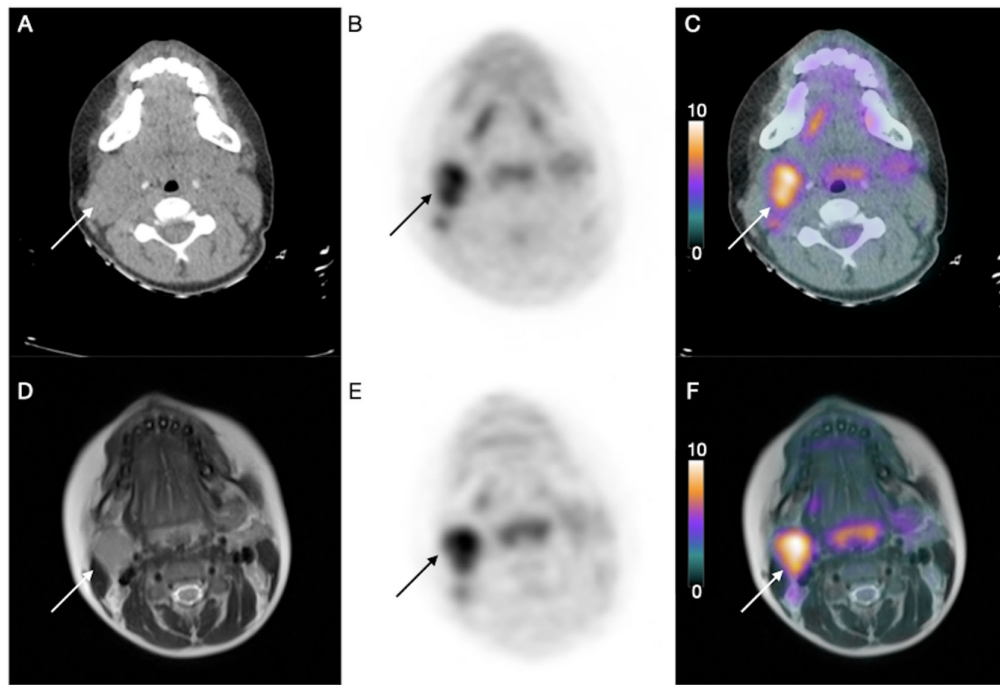


FIGURE 2

Axial CT (A),  $^{18}\text{F}$ -FDG PET (B) and fused  $^{18}\text{F}$ -FDG PET/CT (D) images showing right upper deep cervical lymphadenopathy (arrows) in a 12 year old male with lymphocyte predominant Hodgkin lymphoma at staging. Axial T2 HASTE MRI (D),  $^{18}\text{F}$ -FDG PET (E) and fused  $^{18}\text{F}$ -FDG PET/MRI (F) showing the same.

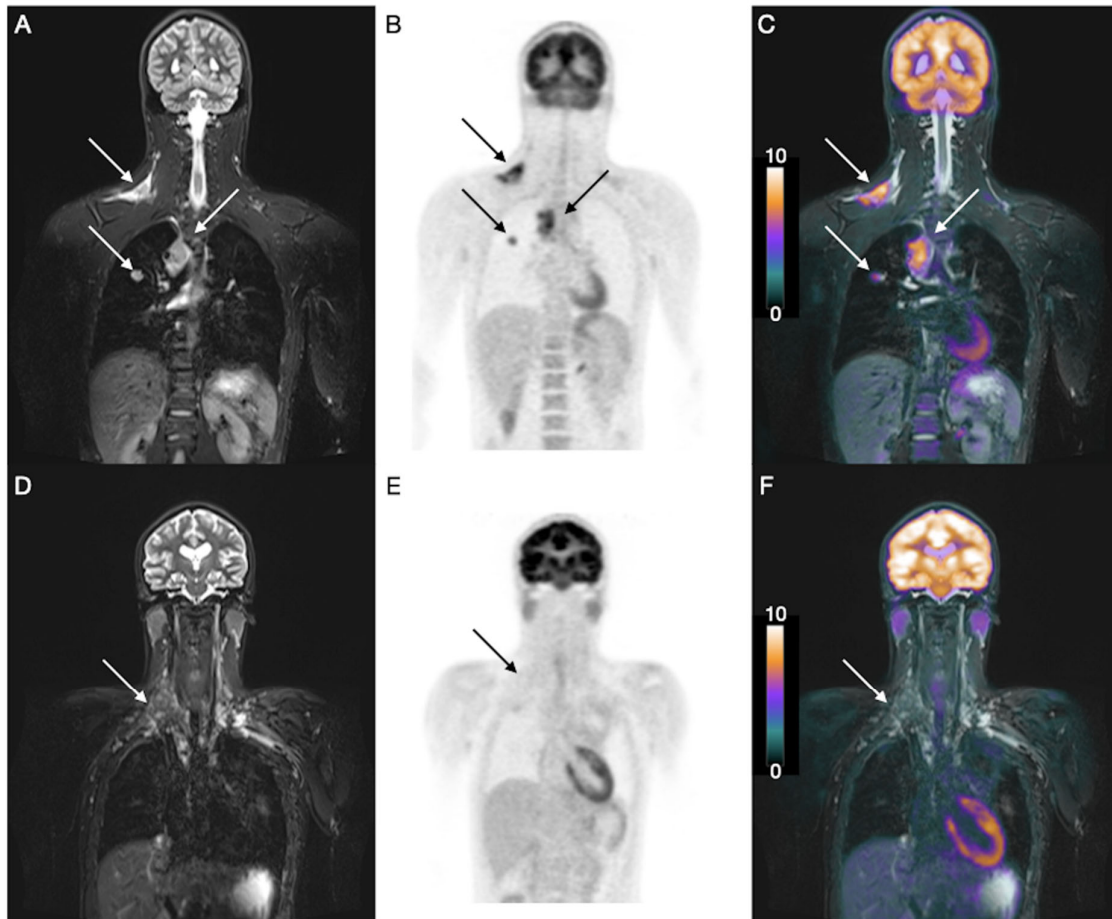


FIGURE 3

A)B)C) Show coronal STIR, <sup>18</sup>F-FDG PET and <sup>18</sup>F-FDG PET/MR fused images demonstrating right supraclavicular fossa and right paratracheal lymphadenopathy, and a right lung nodule (arrows), in a 14 year old male with Hodgkin lymphoma.

D)E)F) Early response assessment following 2 cycles of chemotherapy shows residual, smaller right supraclavicular fossa lymphadenopathy (on D, coronal STIR), with no uptake (on E and F, coronal <sup>18</sup>F-FDG PET and fused <sup>18</sup>F-FDG PET/MR (arrows)). The other sites of disease have resolved.

# GRAPHICAL ABSTRACT

